SIMULATION OF LONG-TERM TRENDS IN CHESAPEAKE BAY EUTROPHICATION

By Carl F. Cerco,[1] Associate Member, ASCE

ABSTRACT: A predictive mathematical model was employed to examine trends in Chesapeake Bay eutrophication from 1959 to 1988. The model provided details of processes and substances for which no record existed. The simulation indicated the volume of anoxic water was largest in the decade 1969–78. Since then, anoxic volume has declined. The decline was largely due to hydrodynamic effects. In 1969–78, high runoff caused the Bay to be highly stratified and inhibited oxygen transport to bottom waters. Less runoff in the years 1979–88 diminished stratification and allowed enhanced oxygen transport to bottom waters. When only years of similar stratification were compared, an increase in anoxic volume was noted from the 1959–68 decade to the 1979–88 decade. The increase was associated with increasing nitrogen concentration in runoff from two major tributaries and with increasing chlorophyll concentration in the mainstem Bay.

INTRODUCTION

Environmental change, natural and man-induced, is at the forefront of environmental research. Identification and interpretation of environmental changes are hampered, however, by the nature of long-term data sets. Observations are often sporadic and subject to methodological inconsistencies. Interpretation of incomplete data leads to controversial, potentially spurious, results. We illustrate a method for detection and interpretation of trends that eliminates many of the problems associated with long-term data sets. Our method supplements observations with application of a predictive mathematical model. This approach offers multiple advantages. Since the model represents the historic record continuously in space and time, no techniques are required to fill gaps in observations. Neither are statistical analyses necessary to distinguish trends from random sampling error. A significant advantage is that the model provides information for which no long-term observations exist.

The approach is demonstrated by simulation of eutrophication trends in Chesapeake Bay. Chesapeake Bay is a classic example of an estuary in distress. Decline in fisheries, loss of submerged aquatic vegetation, and increase in bottom-water anoxia have all been linked to eutrophication trends. To examine these trends, we applied a three-dimensional model package (Cerco and Cole 1993) that included a hydrodynamic model, a water-column eutrophication model, and a benthic sediment submodel.

DATABASE

Dissolved oxygen and chlorophyll observations have been collected in the Bay since the mid 1930s. An assembled data set containing these observations was provided by the USEPA Chesapeake Bay Program Office (CBPO). All data were validated by the CBPO, sometimes by reference to original field records. We appended to the historic record monitoring data from 1984 to 1987, also supplied by the CBPO. A 30-year period, 1959–88, was selected for analysis. The initial year was the earliest for which we could reliably estimate loads to the system. At project commencement, 1988 was the most recent year for which observations were available.

The number of annual observations within the selected period was highly variable. Dissolved-oxygen observations in the historic record were fewer than in the monitoring program and concentrated in summer in the upper half of the bay. Chlorophyll observations were absent in several years in the historic record.

MODEL APPLICATION

Hydrology and Hydrodynamics

The Susquehanna River contributes 62% of the gauged flow to Chesapeake Bay. Consequently, Susquehanna runoff is a prime determinant of circulation and density stratification in the mainstem. The Susquehanna hydrograph is a good surrogate for a hydrograph of total runoff to the system. Examination of the Susquehanna hydrograph for 1959–88 (Fig. 1) indicates flows

[1]Res. Hydro., Mail Stop ES-Q, USACE Wtrwy. Experiment Station, 3909 Halls Ferry Rd., Vicksburg, MS 39180.

Note. Discussion open until September 1, 1995. To extend the closing date one month, a written request must be filed with the ASCE Manager of Journals. The manuscript for this paper was submitted for review and possible publication on August 6, 1993. This paper is part of the ***Journal of Environmental Engineering***, Vol. 121, No. 4, April, 1995. ©ASCE, ISSN 0733-9372/95/0004-0298–0310/$2.00 + $.25 per page. Paper No. 6732.

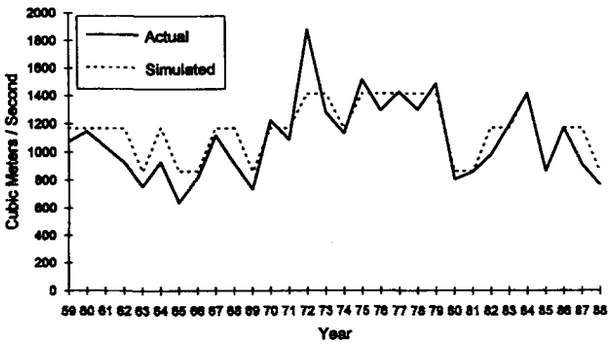

FIG. 1. Actual and Simulated Susquehanna River Hydrology

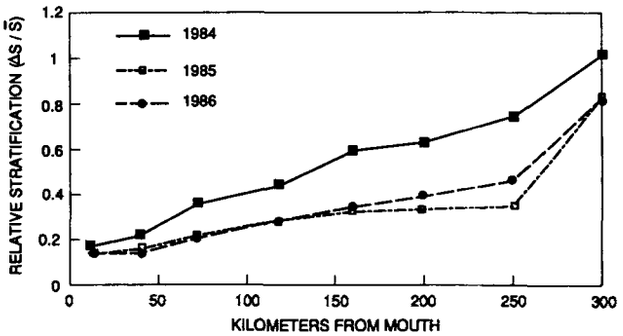

FIG. 2. Observed Relative Stratification in 1984, 1985, 1986

for 1959–68 were mostly at or below the mean flow of 1,087 m^3 sec^{-1}. The period 1959–68 can be characterized as a "dry" decade. Nine out of 10 years in the period 1969–78 were at or above the mean flow. The years 1972 and 1975 were the number one and two highest flows in the period of record (1900–89). The period 1969–78 can be characterized as a "wet" decade. Flows in the period 1979–88 were uniformly distributed above and below average. No distinct characterization is appropriate for this period.

Computation of a 30-year hydrodynamic record exceeded the capacity of the largest supercomputer. Instead, hydrodynamics were approximated by sequencing the annual hydrodynamic series produced for the 1984–86 model calibration. Years in the period 1959–88 were classified as "wet," "average," or "dry" based on annual flow in the Susquehanna. Wet years were at or above the 75th percentile of annual flows in the period of record. Average years were between the 25th and 75th percentile. Dry years had flows below the 25th percentile. Mean flow for 1984, 1,410 m^3 sec^{-1}, exceeded flow for 90% of the years on record. Consequently, 1984 hydrodynamics were employed for "wet" years in the 30-year simulation. Mean flow for 1986, 1,168 m^3 sec^{-1}, was at the 60th percentile in the period of record. Hydrodynamics from 1986 were used to represent "average" years in the simulation. Flow in 1985, 863 m^3 sec^{-1}, was less than 80% of years in the period of record. Modified 1985 hydrodynamics were employed for most "dry" years in the simulation. The modification removed from the "dry" hydrodynamics a November storm that flooded the western tributaries and, to a lesser extent, the Susquehanna. Actual hydrodynamics including the storm were employed for 1985.

Summer salinity stratification provided a key distinction in the hydrodynamics. During 1984, high freshwater runoff in spring induced stratification roughly double 1985 or 1986 (Fig. 2). The "wet" hydrodynamics also qualified as "highly stratified." Despite the distinction as "dry" and "average," little stratification difference existed between 1985 and 1986. Both these years were classified as "normally stratified."

The hydrodynamic sequencing was appropriate to the objective of trend detection. Since individual hydrodynamics were not employed for each of the 30 years, the simulation was not expected to exactly reproduce water quality within a year. The simulation was expected to reproduce trends, however, and to distinguish the influences of hydrology on eutrophication.

Loads

Execution of the model required a 30-year loading sequence of nitrogen, phosphorus, and carbon species corresponding to model state variables (Cerco and Cole 1993).

Point Sources

A listing of point-source facilities and loads for 1965, 1970, and 1980 was provided by the CBPO. We supplemented this record with 1985 point-source loads employed in the model calibration. Transitions from one set of loads to the next were handled as step functions timed to coincide with treatment upgrades at the Washington, D.C., Blue Plains facility, the largest point source in the system.

Fall-Line Loads

Daily fall-line loads were computed as the product of flow and concentration. Concentrations were estimated by a minimum-variance-unbiased-estimator (MVUE) method (Cohn et al. 1989) using a program supplied by the United States Geological Survey (USGS). The program used least-squares techniques to estimate parameters in an equation that related concentration to flow, season, and time

$$\ln(C) = a_1 + a_2(\ln Q - \ln Q_c) + a_3(\ln Q - \ln Q_c)^2 + a_4(t - t_c) + a_5(t - t_c)^2 + a_6 \sin[2\pi(t - 1980)] + a_7 \cos[2\pi(t - 1980)] \quad (1)$$

where C = concentration; Q = volumetric flow rate; Q_c = an arbitrary flow at the center of the range of flows; t = time in decimal years; t_c = an arbitrary time near the center of the range of times; and $a_1, \ldots, a_7$ = constants that relate concentration to flow, season, and time.

Observations employed in the MVUE were also provided by the USGS. Concentration observations were collected by the USGS and CBPO commencing in 1978 to 1980, depending on tributary, and extending to 1990. We added supplementary data (Guide and Villa 1972) collected in 1969–70 at the Susquehanna and Potomac fall lines.

Temporal trends in fall-line concentration were identified through the MVUE program. The program noted the statistical significance of terms in (1). Trends were indicated when the terms containing $(t - t_c)$ and $(t - t_c)^2$ contributed significantly to the least-squares concentration estimate. Increasing nitrogen concentration, primarily in the form of nitrate, was detected in the two largest freshwater sources, the Susquehanna and Potomac Rivers. Both rivers indicated a decrease in dissolved phosphate although only the Potomac demonstrated a decrease in total phosphorus. Trends in the James, the third major freshwater source, were opposite the two larger tributaries; the James demonstrated a decrease in nitrogen and an increase in phosphorus. Concentration trends detected at the three major fall lines are summarized in Table 1.

Extrapolation of concentration trends outside the period of record provided dubious results. Prior to the earliest fall-line observations, the trend terms in the concentration relationship were held constant.

Below-Fall-Line and Atmospheric Loads

Below-fall-line non-point-source loads were specified on a seasonal basis. Loads were derived from output of a predictive watershed model (Donigian et al. 1991). Watershed model loads were available for 1984–86. From these, load-runoff relationships were created for each below-fall-line watershed. Next, a 30-year record of flow in each watershed was constructed by ratio relationships to long-term gauge records. The flow records were employed in the load-runoff relationships to determine a 30-year time series of non-point-source loads.

Non-point-source loads for 1984–86 determined from the load-runoff relationships were compared to the original loads from the watershed model. Over 3 years, total loads in each watershed estimated by the two methods were virtually identical. Differences occurred in individual seasons, however. Median difference was 22% for seasonal total nitrogen loads, 42% for seasonal total phosphorus loads, and 57% for seasonal total organic carbon loads.

Contemporary atmospheric nutrient loads to the water surface were applied throughout the simulation. In all likelihood, both below-fall-line and atmospheric loads have increased over 30 years but no means exists to compute the increase. Omission of temporal trends in these loads is of minor importance, however, since the combined contribution of below-fall-line and atmospheric loads is presently less than 25% of total loading.

Load Summary

Load-reduction scenarios showed eutrophication processes were insensitive to external loads of oxygen-demanding material, except in the immediate vicinity of major load sources. Carbon formed internally, through primary production, was by far the dominant source of oxygen demand in the system. Consequently, load summaries focus on nutrients that support primary production.

Total nitrogen loading to the bay system showed no monotonic trend (Fig. 3). Rather, nitrogen loading was strongly correlated to hydrology. Loading was low in the dry years and high in the wet years. Maximum, virtually equal, loads occurred in 1972 and 1979, the first and third greatest flow years in the series. Minimum load was in 1965, the lowest-flow year in the 30-year series. Virtually all the variation in load was contributed by the fall-line and below-fall-line loads.

TABLE 1. Concentration Trends at Major Fall Lines

Substance (1)	Susquehanna (2)	Potomac (3)	James (4)
Nitrate	0.33 gm m^{-3} increase from 1969 to 1988	0.26 gm m^{-3} increase from 1969 to 1988	0.074 gm m^{-3} decrease from 1979 to 1988
Total Kjeldahl nitrogen	0.085 gm m^{-3} increase from 1969 to 1988	No change	No change
Dissolved phosphate	0.04 gm m^{-3} decrease from 1969 to 1988	0.05 gm m^{-3} decrease from 1969 to 1988	0.064 gm m^{-3} increase from 1979 to 1988
Total phosphorus	No change	0.07 gm m^{-3} decrease from 1969 to 1988	0.095 gm m^{-3} increase from 1979 to 1988

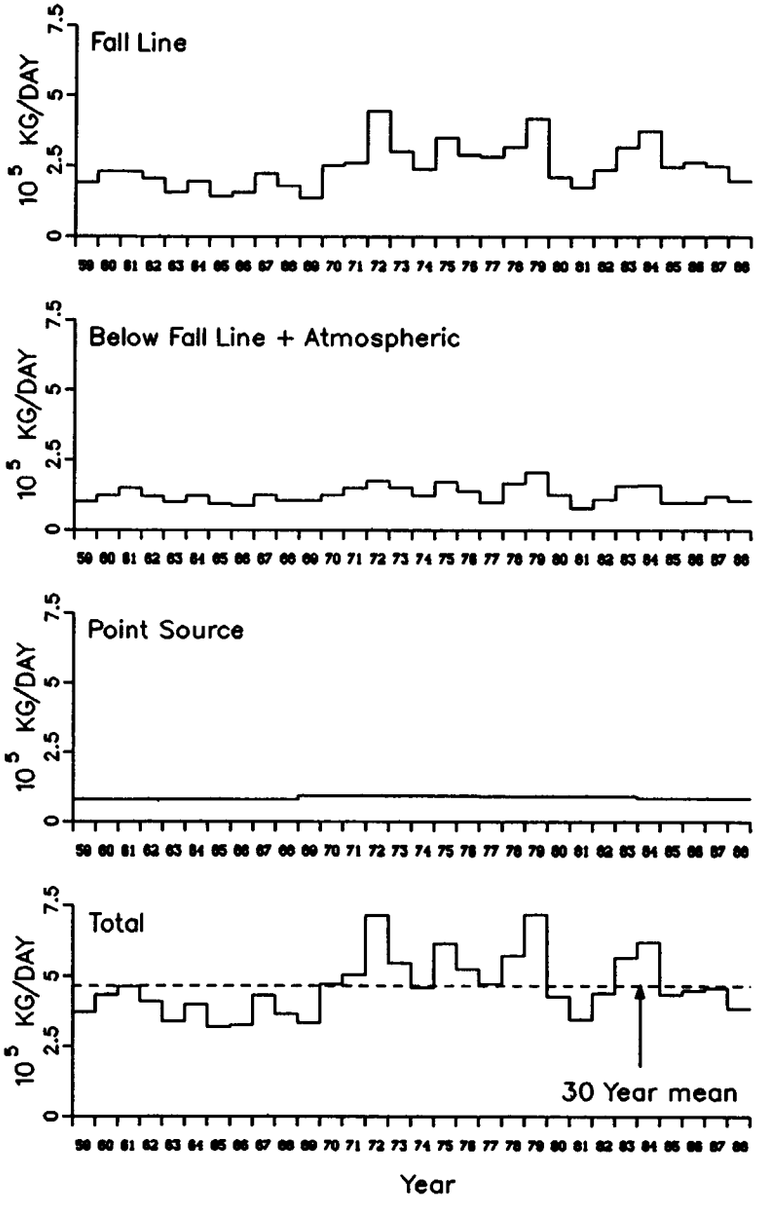

FIG. 3. Total Nitrogen Loads to Chesapeake Bay System: 1959–88

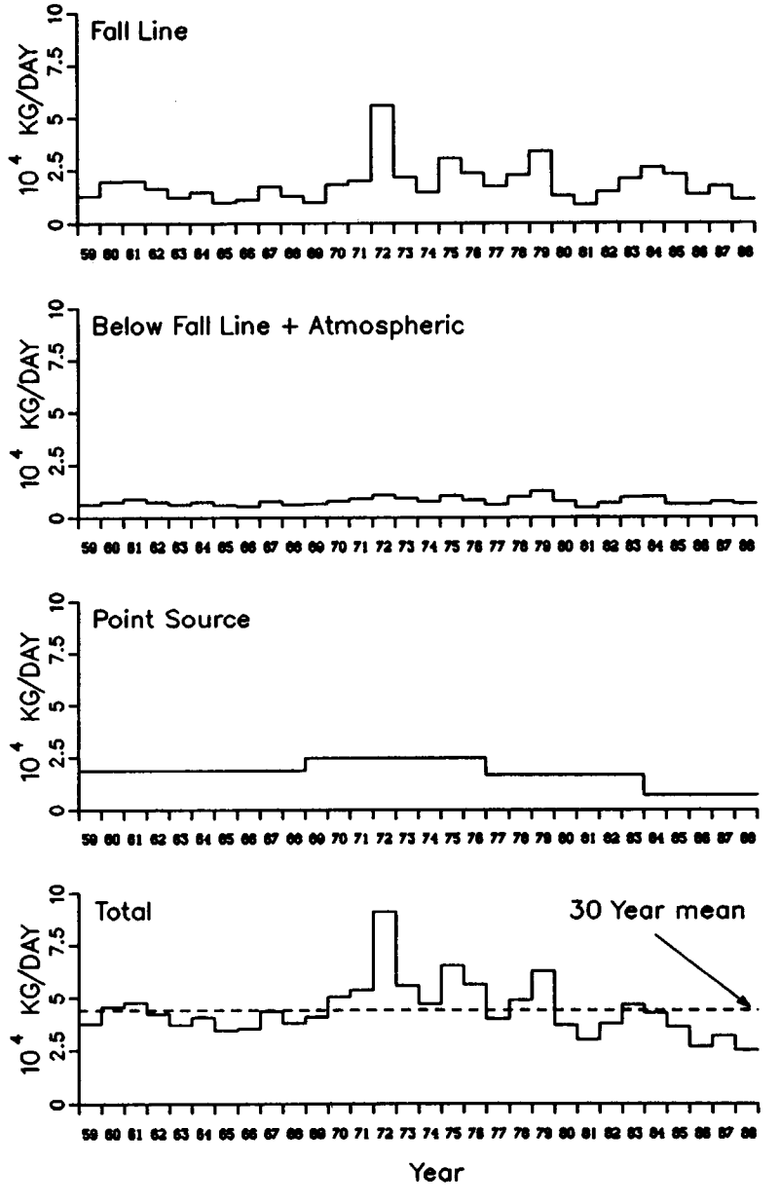

FIG. 4. Total Phosphorus Loads to Chesapeake Bay System: 1959–88

Variation in point-source loads was minor although the most recent loads, 1984–88, exceeded the earliest recorded loads. On a decadal basis, nitrogen loads were least, and below long-term average, in 1959–68. Loads were greatest, and above average, in 1969–78. Loads in 1979–88 were between the extremes.

In contrast to nitrogen, total phosphorus loads to the Bay indicated a long-term trend (Fig. 4). Phosphorus loads peaked in 1972, the year of Tropical Storm Agnes. Loads decreased, with some annual variation, from then to the end of the simulation period. Also in contrast to nitrogen, a large portion of the variation in total phosphorus loads was due to the point-source fraction. Point-source loads from 1984 onward were the least in the 30 years. As a result of average to dry hydrology and point-source control, the lowest loads occurred in the last 3 years of the 30-year sequence. On a decadal basis, phosphorus loads peaked during 1969–78. Loads were usually below average and showed little variability in 1959–68. Lowest load by decade occurred in 1979–88 but the range of loading was wider than in 1959–68.

THIRTY-YEAR SIMULATION RESULTS

Spatial and Temporal Aggregation

Sample location and frequency in the historic record were sporadic. Sample locations in the historic and contemporary data bases exhibited little correspondence. Intepretation and presentation of results required aggregation of observations and predictions that provided meaningful summations and allowed for model-data comparison. Analyses followed a pattern established during the model calibration process. The mainstem Bay was divided into eight zones along the longitudinal axis (Fig. 5). A ninth zone encompassed the Tangier Sound region in the eastern portion of the Bay. The Bay was also divided into layers that approximated the surface mixed layer (0 to 6.7 m), the pyncnocline (6.7 to 12.8 m), and a bottom mixed layer (>12.8 m). The year was divided into four seasons: winter (Julian days 0 to 60), spring (day 61 to 150), summer (day 151 to 270), and fall (day 271 to 365). Seasonal, volumetric means of model results in each zone level were compared to arithmetic mean and range of observations.

Model-Data Comparisons

Dissolved Oxygen and Chlorophyll

Dissolved oxygen and chlorophyll were examined as time series within each zone-level, and as longitudinal plots, by season and level, along the main bay axis. Zones 1 and 2 encompassed

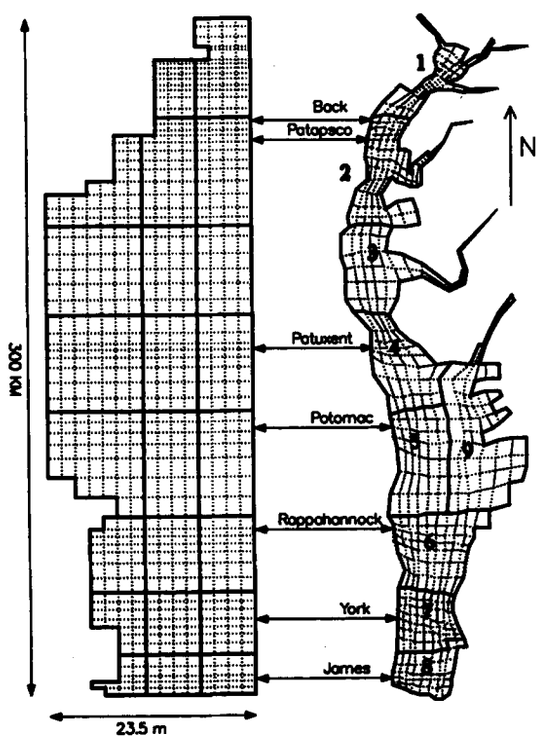

FIG. 5. Zones and Levels for Model and Data Aggregation (Dashed Lines Indicate Individual Model Cells)

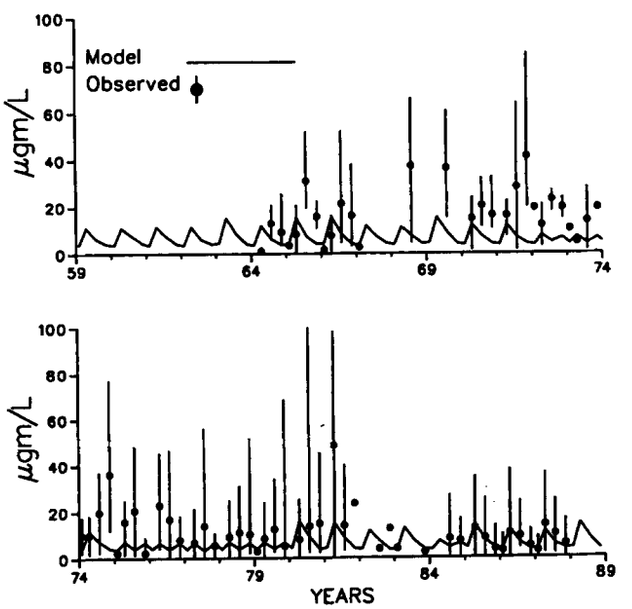

FIG. 6. Observed and Modeled Chlorophyll in Surface of Zone 1, 1959–88, $Z < 6.7$ m

the highest chlorophyll concentrations as well as the greatest number of observations. Time series in these zones (Figs. 6 and 7) revealed enormous observed maximum concentrations in the historic record compared to the monitoring data collected since 1984. In Zone 1, seasonal mean chlorophyll concentrations in the historic record were also much greater than in the contemporary record. In Zone 2, disparity in seasonal mean chlorophyll between historic and contemporary conditions was less noticeable although mean chlorophyll in the years 1969–73 was apparently greater than under present conditions. In both zones, the model performed well in replicating the monitoring data. In Zone 2, the model also performed well in reconstructing the historic data except for the peaks between 1969–73. The large mean concentrations observed in Zone 1 between 1964 and 1981 were not reproduced by the model.

Zone 2 consistently exhibited minimum bottom dissolved oxygen and was a region of high data density. Observed summer-average dissolved oxygen was usually greater during 1959–68 than in subsequent years (Fig. 8). Least summer-average dissolved oxygen occurred in 1973 and in 1976. Close examination of the data indicated minimum dissolved oxygen was greater than zero until 1968. Since then, strictly anoxic conditions were regularly observed. The model performed well in capturing the trends apparent in the data. In particular, predicted dissolved oxygen was greater in the average to dry years (e.g. 1959–68) than in the wet years (e.g. 1973, 1976, 1984).

Summer surface chlorophyll and bottom dissolved oxygen along the bay axis are shown for 3 years, selected based on hydrology and data extent (Fig. 9). The year 1965 was a dry year in a dry decade and was simulated using 1985 hydrodynamics. The year 1976 was a wet year in a wet decade and was simulated using 1984 hydrodynamics. The year 1986 was an average year in a decade of mixed hydrology and was simulated using 1986 hydrodynamics. In the lower 250 km of the bay, agreement between predictions and observations in the historic years, 1965 and 1976, is comparable to agreement in 1986, one of the years to which the model was calibrated. The model corresponds to observations that dissolved oxygen in the deep trench (km 100 to 250) was less in 1976, a wet year, than in dry (1965) to average (1986) years. Above km 250, in Zone 1, observations indicate higher surface chlorophyll and bottom dissolved oxygen in the historic years than in the most recent year. The distinction in Zone 1 between the historic and contemporary observations is not replicated in the model.

Decadal performance summaries, employing previously defined statistics (Cerco and Cole 1993), were prepared using the aggregated observations and model results. (Tables 2 and 3). No trend was apparent in mean dissolved-oxygen error, nor was mean error in the 30-year simulation distinctly different from mean error evaluated for the 3-year model calibration. Mean chlorophyll error for 20 years, 1969–88, was consistent with the calibration but increased by an order of magnitude in the earliest decade. For both substances, absolute mean and relative error in the 30-year simulation increased as a function of time into the past. Magnitude of these two error statistics exceeded values calculated for the model calibration. Exceedence was minor,

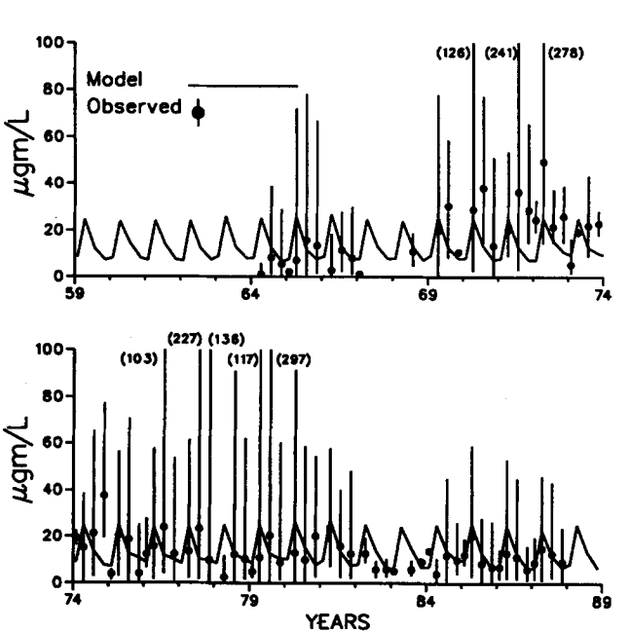

FIG. 7. Observed and Modeled Chlorophyll in Surface of Zone 2, 1959–88, $Z < 6.7$ m

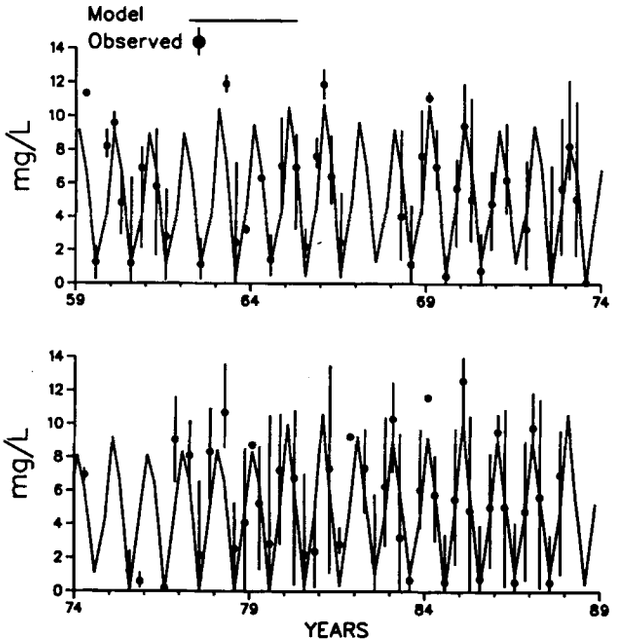

FIG. 8. Observed and Modeled Dissolved Oxygen in Bottom of Zone 2, 1959–88, 12.8 m $< Z$

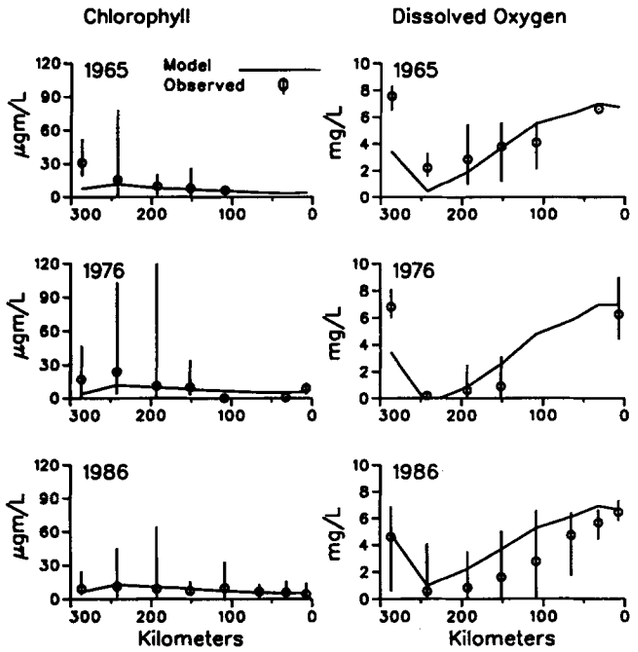

FIG. 9. Observed and Modeled Surface Chlorophyll and Bottom Dissolved Oxygen along Bay Axis: 1965, 1976, 1986

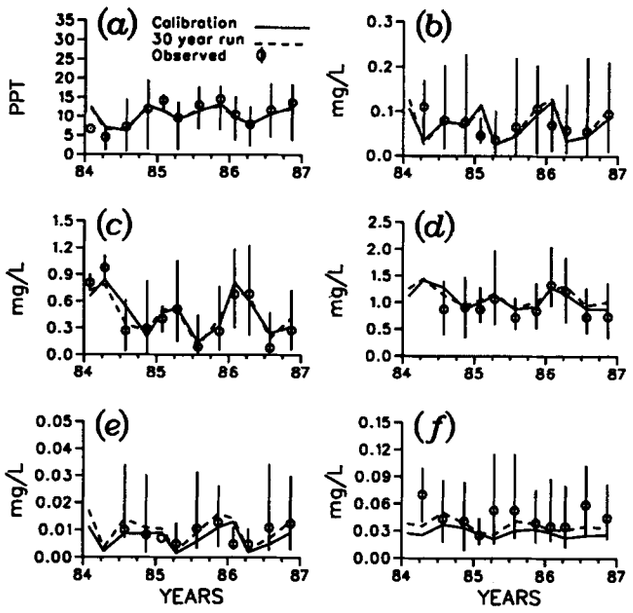

FIG. 10. Comparison of: (a) Salinity; (b) Ammonium; (c) Nitrate; (d) Total Nitrogen; (e) Dissolved Phosphate; (f) Total Phosphorus from 30-Year Run and 3-Year Calibration (Model and Observations from Surface Layer of Zone 2)

TABLE 2. Dissolved Oxygen Performance Statistics

(1)	Mean error ($mg\ L^{-1}$) (2)	Absolute mean error ($mg\ L^{-1}$) (3)	Relative error (%) (4)	Number of observations (5)
Calibration	−0.49	1.14	14.5	10,314
1979–88	−0.67	1.32	16.5	18,951
1969–78	−0.73	1.32	16.3	6,604
1959–68	−0.29	1.57	20.0	5,050

TABLE 3. Chlorophyll Performance Statistics

(1)	Mean error ($\mu g\ L^{-1}$) (2)	Absolute mean error ($\mu g\ L^{-1}$) (3)	Relative error (%) (4)	Number of observations (5)
Calibration	−0.37	3.28	40.6	3,167
1979–88	−0.23	3.59	41.6	6,487
1969–78	−0.31	7.13	72.9	1,443
1959–68	−3.96	9.20	143.0	634

however, for dissolved oxygen and for chlorophyll, 1979–88, but substantial for chlorophyll, 1959–78.

Comparison to 3-Year Simulation

Reliable historic salinity and nutrient observations were not available. An indication of model performance for these substances was obtained by comparison of model output for the years 1984–86 in the 30-year simulation with model calibration results for the same years. Results of the calibration and 30-year simulation agreed well (Fig. 10). The comparison confirmed that the computed historic load sequence allowed realistic predictions of concentration within the bay.

Thirty-Year Time Series

Results of the 30-year simulation were first examined as concentration time series in the mainstem Bay. Annual and summer volumetric means were produced for all model constituents except chlorophyll and dissolved oxygen. Since chlorophyll occurs primarily in the photic zone, chlorophyll concentration was averaged in the surface layer (depth < 6.7 m) only. Since dissolved oxygen depletion occurs primarily in bottom waters, dissolved oxygen was averaged in the bottom layer (depth > 12.8 m) only.

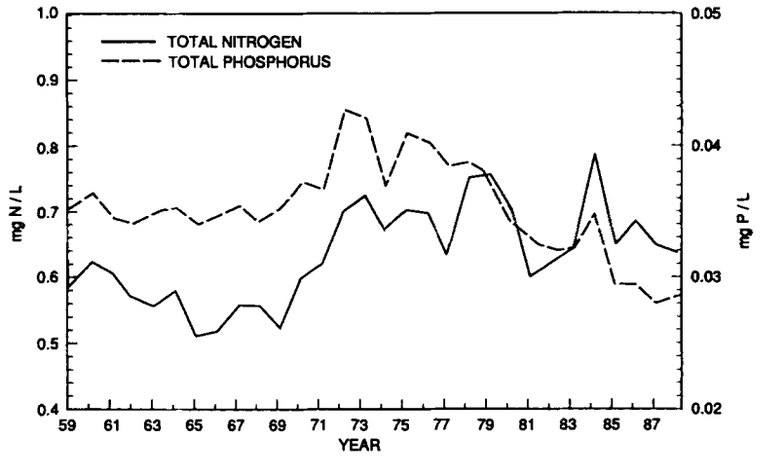

FIG. 11. Annual-Average Total Nitrogen and Phosphorus Concentration in Mainstem Bay, 1959–88

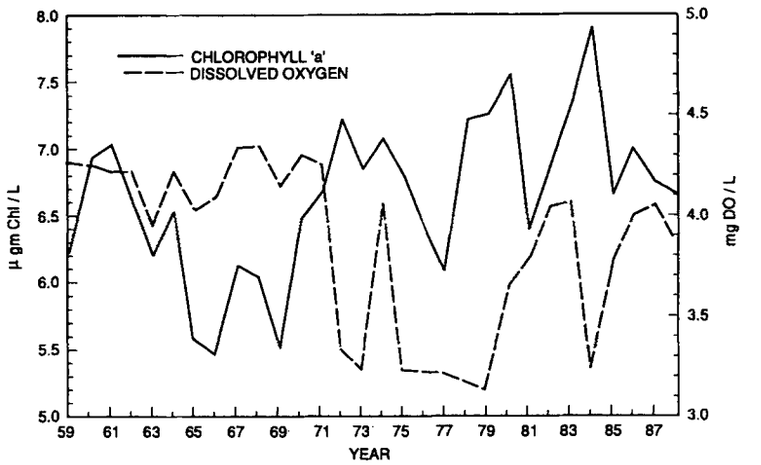

FIG. 12. Summer-Average Surface Chlorophyll and Bottom Dissolved Oxygen in Mainstem Bay, 1959–88

Two influences dominated long-term total nitrogen concentration (Fig. 11). The first was hydrology. Greater concentrations occurred in wet years with high runoff. Minimum total nitrogen was in dry years 1965–69. The second influence was the increasing nitrogen concentrations at the two largest fall lines. As a result of increasing concentration, total nitrogen at the end of the simulation was higher, ≈ 0.06 gm m^{-3} on an annual basis, than at the beginning.

Annual average total phosphorus (Fig. 11) exhibited peak concentrations in 1972 and 1973, concurrent with and following the record runoff that occurred in 1972 during Tropical Storm Agnes. Following the storm, total phosphorus generally decreased through the end of the simulation. Phosphorus was affected by point-source loads as well as hydrology. Point-source loads peaked in 1969–76 and were at the 30-year minimum in years 1984–88. As a result of point-source and non-point-source controls, on an annual basis, total phosphorus declined by ≈ 0.006 gm m^{-3} from beginning to end of the simulation.

Summer-average chlorophyll concentrations (Fig. 12) mirrored the behavior of nitrogen. Chlorophyll concentrations were minimum in 1965–69, years of average to dry hydrology, and higher during wet years. As with nitrogen, chlorophyll concentration was greater at the end of the simulation, ≈ 0.04 mg m^{-3}, than at the beginning. Baywide mean chlorophyll concentration did not reflect the decline in phosphorus concentration from 1972 to the end of the simulation.

During summer, bottom dissolved oxygen (Fig. 12) was closely related to hydrology. Wet years had the least dissolved oxygen as a result of strong stratification and runoff-induced loads. Least summer-average bottom dissolved oxygen in the 30-year series was in 1979, a wet year at the end of a wet decade. No clear trend was evident but summer-average bottom dissolved oxygen at the end of the simulation was ≈ 0.25 gm m^{-3} less than at the beginning of the simulation.

Analysis by Decade

Analysis of simulated time series was subject to pitfalls similar to analysis of observed time series. Although observational uncertainty was absent in the simulation, distinction and analysis

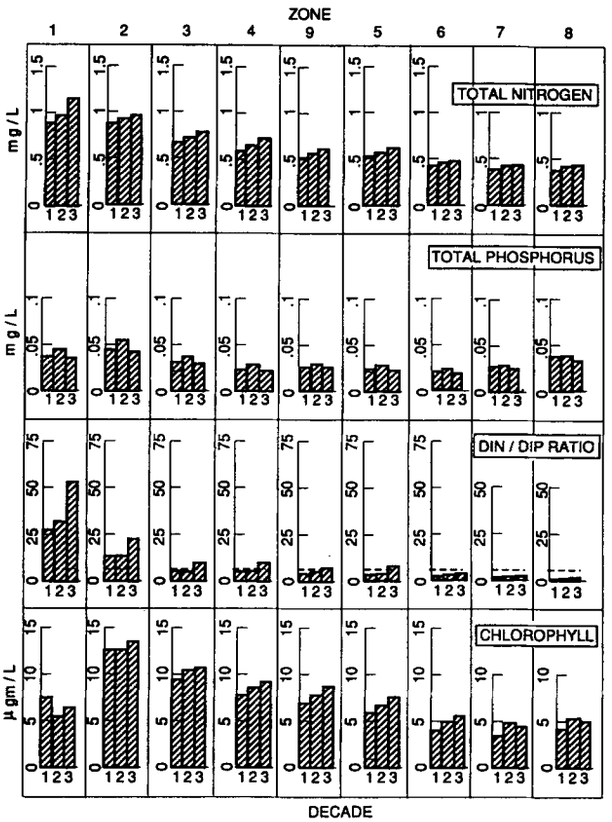

FIG. 13. Surface Total Nitrogen, Total Phosphorus, DIN/DIP Ratio, and Chlorophyll by Zone, Decade (Dashed Line Indicates Redfield DIN/DIP Ratio)

of trends was still obscured by deterministic variability caused by variations in loading and hydrology. An improved picture resulted when simulation results were aggregated by decade for summer only. Summer was selected since it is the season of critical water quality, as evidenced by bottom-water anoxia.

On a decadal basis, summer total nitrogen (Fig. 13) increased monotonically over the three decades. The increase was most noticeable near the Susquehanna fall line. This result was surprising since total nitrogen loads in 1979–88 were less than the preceding decade. Results were clarified when we recalled that runoff-induced nitrogen loads that dominate the total arrive in spring and fall rather than summer. The upward concentration trend at the Susquehanna and Potomac fall lines acted throughout the year, however, and was more influential than total loading in determining summer, baywide nitrogen concentration.

In Zones 1 through 4 and in Zone 9, total phosphorus correlated with decade-averaged loads (Fig. 13). Phosphorus was highest during 1969–78 and less in the preceding and subsequent decades. Little difference among decades was noted downstream of Zones 4 and 9.

Increasing summer nitrogen loads and decreasing phosphorus loads combined to substantially increase dissolved-inorganic-nitrogen (DIN) to dissolved-inorganic-phosphorus (DIP) ratios in surface waters (Fig. 13). The simulation revealed surface waters in Zones 1 and 2 have been phosphorus limited, relative to Redfield stoichiometry, since the 1959–68 decade. The limitation leaped during the 1979–88 decade. Zones 3 through 5 and 9 were nitrogen limited during 1959–78 but approached phosphorus limitation in the most recent decade. Downstream of Zone 5, the Bay was and remains strongly nitrogen limited.

In surface waters throughout most of the Bay, summer chlorophyll (Fig. 13) attained its maximum in the decade 1979–88. Increasing chlorophyll concentration correlated with increasing summer nitrate concentrations at the Susquehanna and Potomac fall lines. Hydrodynamic effects predominated in Zone 1, however, immediately below the Susquehanna fall line. Simulated chlorophyll was highest in the driest decade, 1959–68, least in the wettest decade, 1969–78, and moderate in the decade of variable flows, 1979–88.

The most significant dissolved oxygen variations occurred in the bottom layer of Zones 2 through 4 and Zone 9 (Fig. 14). These included the regions that showed the lowest average dissolved oxygen in the historic record. Simulation results indicated 1959–68 was the decade of highest dissolved oxygen in these regions. The years 1969–78 were the worst decade. Conditions improved in the decade 1979–88 but not to levels in the first decade. A tentative conclusion was that bottom-water dissolved oxygen improved by a small amount, $\approx 0.5\ gm^{-3}$, in the most

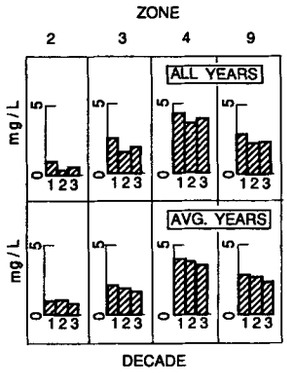

FIG. 14. Bottom Dissolved Oxygen in Upper Bay by Zone, Decade

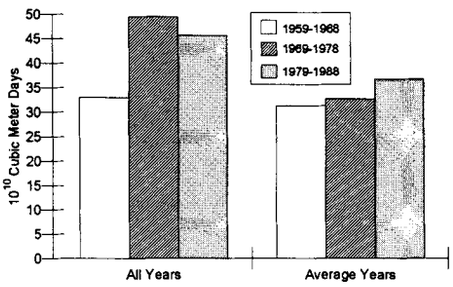

FIG. 15. Anoxic Volume Days by Decade

recent decade. The initial conclusion did not explain the origin of the improvement, however. Was the improvement due to diminished nutrient loads or changes in predominant hydrodynamics in the decade 1979–88 relative to 1969–78? The answer to the question was obtained by comparing only "average" hydrologic years in each decade. Comparison of average years eliminated effects of stratification from the analysis and mitigated the influence of flow-driven load events. Analysis of average years indicated a steady, monotonic decline in bottom-water dissolved oxygen (Fig. 14) from the Back to Rappahannock Rivers and in Tangier Sound. The decadal change was minimal, however: less than 0.3 gm m^{-3} from 1959–68 to 1979–88. The analysis indicated that improvement in dissolved oxygen from 1969–78 to 1979–88 was primarily due to hydrodynamic effects rather than load effects.

Anoxic Volume Days

To compare the occurrence of anoxia among decades, a statistic was created that combined the volume of anoxic water and the duration of the anoxic period. Anoxic water was considered to be water with dissolved oxygen concentration less than 1 gm m^{-3}. The "anoxic volume days" statistic was defined

$$AVD = \sum_{i=1,j=1}^{n,m} V_i \Delta t_j \quad \text{if DO} \leq 1 \tag{2}$$

where AVD = anoxic volume-days (m^3 day); V_i = volume of model cell (m^3); Δt_j = finite-difference integration time step (day); DO = dissolved oxygen concentration (gm m^{-3}); n = number of model cells; and m = number of time steps in year.

Trends in anoxic volume (Fig. 15) mirrored trends in dissolved-oxygen concentration. The decade 1959–68 had the least anoxic volume; the decade 1979–88 had the most. Analysis of years of average hydrology only, however, indicated anoxia increased steadily in the Bay throughout the three decades. In years of average hydrology, anoxic volume was ≈18% greater in 1979–88 than in 1959–68.

HYDRODYNAMICS OR LOADS?

The simulation indicated strong correlation between hydrology and anoxia. The "wet" hydrodynamic years were distinguished by dissolved-oxygen minimal (Fig. 12). The wettest decade, 1969–78, had the largest anoxic volume (Fig. 15). Two factors combined to make wet years high in anoxia. First, large runoff-induced nutrient loads at and below the fall lines promoted algal production. A portion of this production settled to the bottom, decayed, and consumed dissolved oxygen. Second, the water column was more stratified in wet years (Fig. 2). Strong stratification prevented diffusion to the bottom of oxygen in surface water. The fundamental question that arose from the analysis was: "Which of the two processes is most important in creating bottom-water anoxia?" A special model run provided the answer to that question. All loads were left as in the 30-year simulation but 30 years of average, 1986, hydrodynamics were employed.

Comparison of the "wet-dry-average" simulation with the "average only" simulation indicated stratification was the major determinant of anoxia (Fig. 16). Wet hydrodynamics added 28 × 10^{10} m^3 days of anoxia to the anoxic volume, 33 × 10^{10} m^3 days, that occurred when average, 1986, hydrodynamics were employed. The potential variation in anoxia due to loads alone was indicated by the "average only" simulation. The difference between the most and least anoxic years was 18 × 10^{10} m^3 days. Over 30 years, the maximum variation attributable to loads was only 65% of the anoxia caused by high stratification.

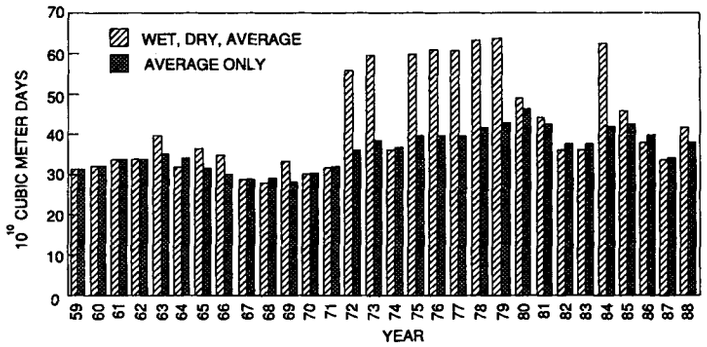

FIG. 16. Effect of Hydrodynamics on Anoxic Volume Days

An unexpected result of the comparison was that dry years exhibited 8×10^{10} m^3 days ($\approx$23%) more anoxia than average years. This result was not explained by stratification since stratification was equivalent in dry and average years (Fig. 2). In a study of Virginia tributaries, Kuo and Neilson (1987) linked anoxia to gravitational circulation. Tributaries with low runoff and weak circulation exhibited more anoxia than the tributary with highest runoff and strongest circulation. They related the phenomenon to residence time. In the presence of weak circulation, water parcels were exposed for a longer period to bottom-oxygen demand. An analogous process apparently occurs in the mainstem Bay. In low-flow periods, circulation is weak and anoxia is greater than in periods of higher flow and strong circulation. In periods of extremely high flow, however, stratification is sufficient to overcome the beneficial effects of strong circulation.

COMMENT

The mean-error statistic described whether the model overestimated or underestimated the observations. Absolute-mean and relative errors were measures of the average difference between predictions and observations. Computation of mean error indicated the simulation reproduced the 30-year dissolved-oxygen record, on average, as well as the monitoring data to which the model was calibrated (Tables 2 and 3). The simulation reproduced chlorophyll, on average, as well over 20 years as over 3 years. Computation of absolute-mean and relative errors indicated agreement between simulated and observed season-zone-level dissolved-oxygen means over 30 years was diminished from the calibration but not substantially. By contrast, agreement of simulated and observed season-zone-level chlorophyll means diminished substantially as a function of time into the past. These performance statistics were influenced by nature of the assembled data set and by inherent limitations in long-term simulations.

Agreement between predictions and observations in each decade, as measured by absolute-mean and relative error statistics, was inversely proportional to the number of observations (Tables 2 and 3). When large numbers of synoptic observations were available, as in 1979–88, superior agreement was obtained between model and observations. Comparison of the model to sporadic data resulted in diminished agreement, in part, because the observations were inferior indicators of conditions in the estuary. The phenomenon was especially noticeable for chlorophyll for which the disparity in number of observations among decades was greatest. The deterioration of data reliability backward in time was one reason the model was employed to provide insights into historic phenomena.

A second factor in diminished agreement backward in time is the occurrence of environmental changes not incorporated in the model. In effect, the input data and calibration parameters become less representative as distance into the past increases. Inspection of the observations and model results indicates changes not represented in the model have occurred. The enormous maximum chlorophyll concentrations observed in the upper bay circa 1969 to 1981 have not been observed in more recent monitoring efforts, 1984–87, despite an increase in sample number and coverage (Figs. 6 and 7). The sporadic nature of the observations blurs conclusions about trends in mean chlorophyll. The decline in maximum concentrations cannot be denied, however. The simulation did not replicate the immense chlorophyll concentrations observed in Zones 1 and 2 during the first two decades. The simulation demonstrated one set of algal growth kinetics is not applicable to the upper Bay over three decades. Alterations in one or more factors affecting algal growth have occurred in the past decade. Changes in algal species induced by nitrogen enrichment have been observed elsewhere in the bay system (Sanders et al. 1987). Species change may have been induced near the Susquehanna as well by effective nitrogen enrichment, as evidenced by the increase in DIN/DIP ratio in the past year (Fig. 13).

Numerous investigators have examined the historic database for Chesapeake Bay and reached disparate conclusions. One of the first data syntheses (Heinle et al. 1980) concluded oxygen concentrations in the Bay had not changed greatly. An alarm was sounded when a subsequent

investigation reported an order-of-magnitude increase in anoxic volume from 1950 to 1980 (Flemer et al. 1983). One investigation reported spring runoff was the primary determinant of anoxia (Seliger and Boggs 1988) while a subsequent analysis found only a weak qualitative link between runoff and anoxic volume (Bahner et al. 1990). The disparate conclusions can be largely traced to the incomplete data base. Synoptic surveys were lacking and investigators were forced into selective employment of the data. Examination of the reconstructed anoxic volume record (Fig. 16) provides insight into the preceding analyses and a more complete picture of actual trends and determining processes.

The year 1980 was preceded by a series of high-runoff years, 1972–79. High stratification and loading in these years resulted in anoxic volume roughly double anoxia in 1959 to 1971 (Fig. 16). In 1980, an investigator would correctly conclude the Bay had grown worse but would not see the origin as primarily transient, high stratification. The increase in anoxic volume could easily be interpreted as a monotonic trend linked to nutrient loads. Our work confirms runoff-induced stratification is the predominant determinant of anoxic volume. The influence of stratification obscures and confounds detection of lesser trends in anoxia attributable to loading. When hydrodynamic effects are removed, our work indicates a small increase in anoxic volume has occurred over two decades. The increase is associated with increasing nitrogen concentration at the two major fall lines and an increase in summer chlorophyll concentration in most of the mainstem Bay.

CONCLUSIONS

Hydrodynamics were the predominant influence on anoxic volume. Anoxic volume induced by high stratification, as in 1984, was 50% greater than the range of load-induced anoxia over the 30-year period. The extreme variation in anoxic volume over 30 years was approximately a factor of two. Highest anoxic volume was in 1979, 64×10^{10} m^3 days. Least anoxic volume was in 1968, 28×10^{10} m^3 days.

Dissolved-oxygen trends in the Bay were subtle and unlikely to be detected solely by analysis of observations. On a decadal basis, dissolved oxygen in the Bay was least during 1969–78. Summer-average bottom dissolved oxygen improved by 0.5 gm m^{-3} in the 1979–88 decade. The improvement was primarily due to hydrodynamic effects, however. When only years of "average" hydrology were compared, bottom dissolved oxygen declined by $\approx$0.3 gm m^{-3} from 1959–68 to 1979–88.

Trends in anoxia were tied to trends in nitrogen concentration in the two major fall lines. Added nitrogen in runoff promotes algal production. Algal biomass settles to the bottom, decays, and consumes oxygen. Phosphorus load reductions since 1972 had no discernable effect on anoxia.

Observations indicate maximum chlorophyll concentration has decreased near the Susquehanna fall line over 30 years. Phosphorus control is suspected as the influence but cannot be confirmed by the present analysis. The region of potential phosphorus control is limited in extent, however. Baywide, the simulation indicates summer chlorophyll concentration is increasing due to an underlying increase in nitrogen concentration at two major fall lines.

ACKNOWLEDGMENTS

The Chesapeake Bay model study was sponsored by the U.S. Army Engineer District, Baltimore, and by the Chesapeake Bay Program Office, Region III, U.S. Environmental Protection Agency. Permission was granted by the Chief of Engineers to publish this information.

APPENDIX I. REFERENCES

Bahner, L., Reynolds, R., and Batuik, R. (1990). "Volumetric analysis of dissolved oxygen trends in the Chesapeake Bay: preliminary findings." *Rep.*, Chesapeake Bay Program, U.S. Environmental Protection Agency, Annapolis, Md.

Cerco, C., and Cole, T. (1993). "Three-dimensional eutrophication model of Chesapeake Bay." *J. Envir. Engrg.*, ASCE, 119(6), 1006–1025.

Cohn, T., DeLong, L., Gilroy, E., Hirsch, R., and Wells, D. (1989). "Estimating constituent loads." *Water Resour. Res.*, Vol. 25, 937–942.

Donigian, A., Bicknell, B., Patwardhan, A., Linker, L., Algre, D., Chang, C., and Reynolds, R. (1991). "Watershed model application to calculate bay nutrient loadings." *Rep.*, Chesapeake Bay Program Office, U.S. Environmental Protection Agency, Annapolis, Md.

Flemer, D., Mackiernan, G., Nehlsen, W., and Tippie, V. (1983). "Chesapeake Bay: a profile of environmental change." *Rep.*, U.S. Environmental Protection Agency, Region III, Philadelphia. Pa.

Guide, V., and Villa, O. (1972). "Chesapeake Bay nutrient input study." *Tech. Rep. 47*, Annapolis Field Office, Region III, U.S. Environmental Protection Agency, Annapolis, Md.

Heinle, D., D'Elia, C., Taft, J., Wilson, J., Cole-Jones, M., Caplins, A., and Cronin, E. (1980). "A historical review of water quality and climatic data from Chesapeake Bay with emphasis on effects of enrichment." *CBP-TR-002E*, Chesapeake Bay Program, U.S. Environmental Protection Agency, Annapolis, Md.

Kuo, A., and Neilson, B. (1987). "Hypoxia and salinity in Virginia estuaries." *Estuaries*, 10(4), 277–283.

Sanders, J., Cibik, S., D'Elia, C., and Boynton, W. (1987). "Nutrient enrichment studies in a coastal plain estuary: changes in phytoplankton species composition." *Can. J. Fisheries and Aquatic Sci.*, Vol. 44, 83–90.
SAS Institute Inc. (1988). *SAS/STAT user's guide, release 6.03 edition*. Cary, N.C.
Seliger, H., and Boggs, J. (1988). "Long-term pattern of anoxia in the Chesapeake Bay." *Understanding the estuary: advances in Chesapeake Bay research*, M. Lynch and E. Krone, eds., Chesapeake Research Consortium, Gloucester Point, Va., 570–585.

APPENDIX II. NOTATION

The following symbols are used in this paper:

AVD = anoxic volume days;
$a_1, \ldots, a_7$ = constants that relate fall-line concentration to flow, season, time;
C = concentration of dissolved substance at fall line;
Q = fall-line volumetric runoff;
Q_c = arbitrary value of fall-line runoff;
$\bar{S}$ = vertically averaged salinity;
t = time;
t_c = arbitrary time near center of time series;
V_i = volume of model cell i;
ΔS = surface-to-bottom salinity difference; and
Δt_j = finite-difference integration item step.